Synthesis and Gas Transport Properties of New High Glass Transition Temperature Ring-Opened Polynorbornenes

Armando Pineda Contreras and Mikhail A. Tlenkopatchev

Instituto de Investigaciones en Materiales, Universidad Nacional Autónoma de México, Apartado Postal 70-360, CU, Coyoacán, México DF 04510, México

Maria del Mar López-González and Evaristo Riande*

Instituto de Ciencia y Tecnología de Polímeros (CSIC), 28006 Madrid, Spain

Received November 12, 2001; Revised Manuscript Received March 12, 2002

ABSTRACT: The synthesis and polymerization of the new monomers *N*-(1-adamantyl)-*exo*-norbornene-5,6-dicarboximide (AdNDI), *N*-cyclohexyl-*exo*-norbornene-5,6-dicarboximide (ChNDI), and *N*-phenyl-*exo*-norbornene-5,6-dicarboximide (PhNDI) are reported. Copolymers of *N*-(1-adamantyl)-*exo*-norbornene-5,6-dicarboximide/norbornene, with molar compositions 50/50, 70/30, and 30/70, were also obtained. The transport of hydrogen, oxygen, nitrogen, carbon monoxide, carbon dioxide, methane, ethylene, and ethane across membranes prepared from these homopolymers and copolymers was determined at 30 °C using permeation techniques. Diffusion coefficients correlate rather well with the diameter of diffusant molecules except in the case of carbon dioxide. The values of the permselectivity coefficient for different gases depend on the type of membranes. For example, the permselectivity of oxygen with respect to nitrogen, $\alpha(O_2/N_2)$, is ca. 5.50 for membranes prepared from *N*-(1-adamantyl)-*exo*-norbornene-5,6-dicarboximide/norbornene (50/50) copolymers, which compares favorably with the values reported for this parameter in membranes with imide groups located in the backbone. The values of $\alpha(H_2/C_2H_6)$ in membranes of poly(*N*-(1-adamantyl-*exo*-norbornene-5,6-dicarboximide), poly(*N*-cyclohexyl-*exo*-norbornene-5,6-dicarboximide), and poly(*N*-phenyl-*exo*-norbornene-5,6-dicarboximide) are 183, 124, and 122, respectively, whereas the values of $\alpha(C_2H_4/C_2H_6)$ amount to 6.9, 7.6, and 6.4, respectively. For most membranes used in this study, diffusion rather than solubility is responsible for the discrimination of gas transport. However, solubility is mainly responsible for the high permselectivity of ethylene with respect to ethane displayed by the membranes.

Introduction

Gas transport in membranes depends on the physical state (glassy, rubbery, or crystalline) of the polymer integrating the barrier membranes. Crystalline regions in semicrystalline polymers are opaque to gas transport whereas micro-Brownian motions in rubbery polymers facilitate nonpermanent holes formation through which the molecules of diffusant can easily jump. The solubility coefficient of gases, *S*, in amorphous rubbery membranes is an increasing function of pressure, and the pressure dependence of *S* can be obtained from the variation of the free energy involved in the mixture of the polymer with the gas in the liquid state.[1,2] Solubility rather than diffusion controls the permselectivity of rubbery membranes.

In the glassy state, the solubility coefficient is a decreasing function of pressure. This behavior is usually interpreted in terms of the dual mode model[3] that considers glassy membranes as a continuum phase in which microvoids or holes that account for the excess volume are dispersed. According to the model, solubility occurring in the continuous phase obeys Henry's law whereas the microvoids act as Langmuir sites where the gas is adsorbed. Gas transport takes place through absorption and adsorption sites, but a failure of the model is that conjugated transport between Henry and Langmuir sites is not considered.[4] Despite these shortcomings, the dual model is commonly used to interpret gas transport in glassy membranes. Recent permeation experiments show that gas transport through linear low-density polyethylene (LLDPE) can also be interpreted in terms of the dual mode model.[5,6]

The separation of oxygen and nitrogen from air for industrial combustion and to prevent oxidation, respectively, is carried out using membranes' technology.[7] Also, this technology is used for the removal of hydrogen from mixtures with nitrogen or hydrocarbons in petrochemical processes.[7] Therefore, it is obvious the importance of correlating gas transport with the chemical structure of the barriers utilized for gases separation. Chain fluctuations that give rise to the formation of channels through which the molecules of diffusant can migrate to a neighboring cavity are severely hindered in the glassy state due to the fact that only local motions are allowed. In the glassy state both diffusion and solubility control gases separation of similar size, but when the sizes of the diffusants largely differ, diffusion may be the controlling step. The information at hand suggests that glassy polymers having bulky side groups in their structure contain large cavities that facilitate gas permeability without negatively affecting the permselectivity. These polymers have in general high glass transition temperatures, and therefore aging processes that might affect gas transport are not important at the temperatures of use. Polycarbonates, polysulfones, polyimides, and poly(ether imide)s are polymers commonly used in gas separation.[7−11]

It is important to devise methods that permit the prediction of the performance of membranes for gas separation as a function of the chemical structure. Molecular dynamics may be an important tool for this task, though its use is restricted to rubbery membranes. Actually, molecules of diffusant spend a large time moving in cavities in glassy membranes so that the

10.1021/ma011959p CCC: $22.00
Published on Web 05/09/2002

computing time necessary to reach the diffusive regime may be prohibitively large. To circumvent this problem, the transition-state approach (TSA) was formulated.[12] The theory assumes that the molecules of gas migrate through polymer structures in a sequence of hops between local minima of the potential. Despite the promising results, some refinements are still necessary in order that the theory can be used for realistic simulation of gas transport in terms of the chemical structure of membranes.[13−16]

Another approach that can be useful for the design of optima membranes for gas separation is to investigate in a systematic way the effect of chemical structure on gas transport. Norbornene monomers are attractive due to their facile functionalization and high reactivity using ring-opening metathesis polymerization (ROMP).[17−19] Polynorbornenes of high molecular weight and good mechanical properties were obtained by ROMP of norbornene monomers[20] using appropriate catalysts. The capability of polynorbornenes for packaging and gas separation has been investigated.[21−25] Gas transport studies in ring-preserved polynorbornenes prepared via addition polymerization route have also been reported.[26,27]

The polymers described in this work contain imide groups in the side chains and it is a purpose of this work to investigate whether the presence of these groups enhances the permselectivity characteristics of polynorbornenes. Thus, polymers obtained from the homopolymerization of *N*-(1-adamantyl)-*exo*-norbornene-5,6-dicarboximide (PAdNDI, M1), *N*-cyclohexyl-*exo*-norbornene-5,6-dicarboximide (PChNDI, M2), and *N*-phenyl-*exo*-norbornene-5,6-dicarboximide (PPhNDI, M3) and from copolymers of *N*-(1-adamantyl)-*exo*-norbornene-5,6-dicarboximide and norbornene (NB) were used for the preparation of membranes. Schematic representations of the repeating units of the polymers are shown in Figure 1. It is worthy to note that the chains contain double bonds in the backbone that confer rigidity to them.

In this work the permeation coefficients of hydrogen, oxygen, nitrogen, carbon monoxide, carbon dioxide, methane, ethane, and ethylene in M1, M2, and M3 as well in the copolymers *N*-(1-adamantyl)-*exo*-norbornene-5,6-dicarboximide/norbornene with molar ratios 50/50 (M4), 70/30 (M5), and 30/70 (M6) were measured with the aim of obtaining information on the permselectivity performance of these materials to gases.

Experimental Part

Materials. *exo*-Norbornene-5,6-dicarboxylic anhydride (*exo*-NDA, **1**) was prepared via Diels−Alder condensation of cyclopentadiene and maleic anhydride and by the thermal isomerization of the corresponding endo isomer according to the literature.[28] 1-Adamantanamine, cyclohexylamine, aniline, and other chemicals were purchased from Aldrich Chemical Co. 1,2-Dichloroethane, dichloromethane, chlorobenzene, and toluene were dried over anhydrous calcium chloride and distilled under nitrogen over CaH_2. $RuCl_3 \cdot xH_2O$ was used as received. $RuCl_2(PPh_3)_3$ and $(PPh_3)_2Cl_2Ru{=}C{=}CH(t\text{-}Bu)$ were prepared according to the literature.[29,30]

Measurements. ^1H NMR and ^{13}C NMR spectra were recorded on a Varian spectrometer at 300 and 75.5 MHz frequencies, respectively, in $CDCl_3$ with tetramethylsilane (TMS) as internal standard.

The glass transition temperatures were measured under nitrogen with a Du Pont 2100 instrument, at a heating rate of 10 °C/min. The samples were encapsulated in standard aluminum DSC pans in duplicate. Each pan was run twice on the temperature range 30−300 °C. FTIR spectra were obtained on a Nicolet 510 p spectrometer.

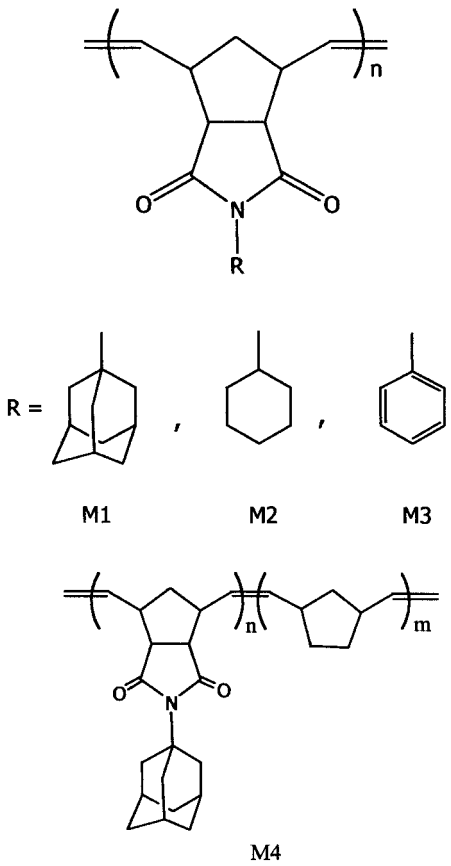

Figure 1. Schematic representation of the repeating units of poly(*N*-(1-adamantyl)-*exo*-norbornene-5,6-dicarboximide) (M1), poly(*N*-cyclohexyl-*exo*-norbornene-5,6-dicarboximide) (M2), poly(*N*-phenyl-*exo*-norbornene-5,6-dicarboximide) (M3), and copolymers of *N*-(1-adamantyl)-*exo*-norbornene-5,6-dicarboximide with norbornene.

Copolymer compositions were determined by ^1H NMR integration of the olefinic peak of *N*-(1-adamantyl)-*exo*-norbornene-5,6-dicarboximide (AdNDI) (5.65 ppm) units relative to the olefinic protons of norbornene units (5.3 ppm). Molecular weights and molecular weight distributions with reference to polystyrene standards were determined with a Varian 9012 GPC instrument at 30 °C in chloroform (universal column and a flow rate of 1 mL min^{-1}).

Membranes were prepared by casting from chloroform solutions. Gas permeation through the membranes was measured at 30 °C using a thermostated experimental device described in detail elsewhere.[13] The diameter of permeation area of the membranes was 1.7 cm. Thicknesses of 110−180 μm, depending on the membrane, were used. The permeation apparatus is made up of a high-pressure or upstream chamber separated from a low-pressure or downstream chamber by the membrane. A pressure sensor MKS of range 10^{-4}−1 mmHg measures the pressure in the downstream chamber, and a pressure transducer Gometrics of 0−10 bar range is used to measure the pressure in the upstream chamber. Vacuum is made in the two chambers, and the gas contained in a reservoir at a pressure close to that to be used in the upstream chamber is allowed to flow suddenly to the downstream chamber. Then the flow of gas from the upstream to the downstream chamber is monitored by the variation of pressure of gas in the latter chamber as a function of time. Before performing each experiment, the inlet of air into the evacuated downstream chamber was measured as a function of time and further subtracted from the curves representing the pressure of permeant against time in the downstream chamber.

Monomers Synthesis. *N-(1-Adamantyl)-exo-norbornene-5,6-dicarboximide (AdNDI,* **3a**). *exo*-NDA **1** (12 g, 70 mmol)

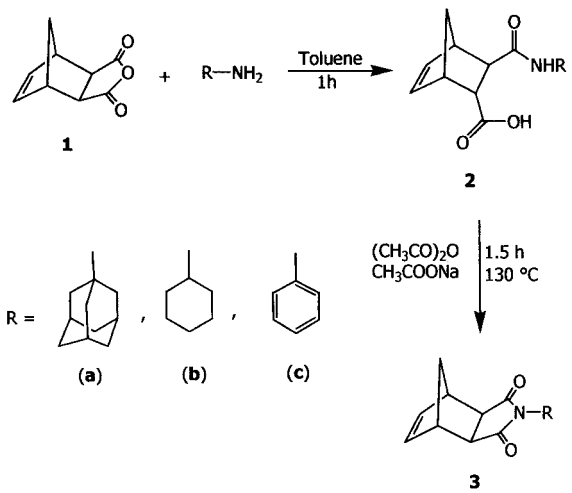

Figure 2. Synthesis of monomers *N*-(1-adamantyl)-*exo*-norbornene-5,6-dicarboximide (**3a**), *N*-cyclohexyl-*exo*-norbornene-5,6-dicarboximide **(3b),** and *N*-phenyl-*exo*-norbornene-5,6-dicarboximide (**3c**).

was dissolved in 120 mL of toluene. 11 g (72 mmol) of adamantanamine in 120 mL of toluene was added dropwise to the stirred solution of *exo*-NDA. The reaction was maintained at 90 °C for 1 h and then cooled to room temperature. A precipitate was filtered and dried to give 22 g (70 mmol) of amic acid. Obtained amic acid **2** (22 g, 70 mmol), anhydrous sodium acetate (3.3 g, 40 mmol), and acetic anhydride (65 g, 640 mmol) were heated at reflux for 2 h and then cooled. The solid crystallized on cooling was filtered, washed several times with water, and dried in a vacuum oven at 50 °C overnight. Pure monomer **3a** (Figure 2) was obtained after twice recrystallization from ethanol: yield = 85%, mp = 159−161 °C. ^{1}H NMR (300 MHz, $CDCl_3$): δ (ppm) = 6.25 (2H, s), 3.22 (2H, d), 2.48 (2H, d), 2.41 (1H, d), 2.11 (1H, s), 1.68−1.72 (1H, m), 1.33−1.44 (1H, d). ^{13}C NMR (75 MHz, $CDCl_3$): δ (ppm) = 181.52, 138.72, 65.94, 52.94, 48.91, 44.53, 42.21, 36.72, 30.76. FT-IR: 3062 (C═C−H str), 2911 (C−H asym str), 2883 (C−H sym str), 1762 (C═O), 1667 (C═C str), 1455 (C−H def), 1337 (═CH− def), 1373 (C−H def), 1290 (C−H def), 1200 (C−N str), 975 (C−C skel), 784 cm^{-1} (C═C−H def).

N-Cyclohexyl-exo-norbornene-5,6-dicarboximide (ChNDI, **3b**). *exo*-NDA **1** (12 g, 70 mmol) was dissolved in 120 mL of toluene. An amount of 7 g (72 mmol) of cyclohexylamine in 120 mL of toluene was added dropwise to the stirred solution of *exo*-NDA. The reaction was maintained at room temperature 1 h. A precipitate was filtered and dried to give 18.6 g (72 mmol) of amic acid **2b**. The amic acid obtained (18.6 g, 72 mmol), anhydrous sodium acetate (3.3 g, 40 mmol), and acetic anhydride (65 g, 640 mmol) were heated at reflux for 2 h and then cooled. The solid crystallized on cooling was filtered, washed several times with water, and dried in a vacuum oven at 50 °C overnight. Pure monomer **3b** (Figure 2) was obtained after twice recrystallization from methanol: yield = 87%, mp = 130−131 °C. ^{1}H NMR (300 MHz, $CDCl_3$) (Figure 3): δ (ppm) = 6.27 (2H, s)**,** 3. 94 (H, m), 3.25 (2H,d), 2.60 (2H, d), 2.12−2.16 (2H, m), 1.79−1.84 (1H, m), 1.46−1.60 (2H, m), 1.33−1.44 (1H, d). ^{13}C NMR (75 MHz, $CDCl_3$): δ (ppm) = 178.19, 137.83, 51.59, 47.38, 45.38, 42.52, 28.74, 25.79, 25.02. FT-IR: 3062 (C═C−H str), 2984 (C−H asym str), 2857 (C−H sym str), 1762 (C═O), 1664 (C═C str), 1465 (C−H def), 1346 (═CH− def), 1370 (C−H def), 1255 (C−H def), 1199 (C−N str), 975 (C−C skel), 784 cm^{-1} (C═C−H def).

N-Phenyl-exo-norbornene-5,6-dicarboximide (PhNDI, **3c**). PhNDI was prepared according to literature.[31] Pure monomer **3c** (Figure 2) was obtained after twice recrystallization from toluene: yield = 81%, mp = 195−196 °C. ^{1}H NMR (300 MHz, $CDCl_3$): δ (ppm) = 7.49−7.25 (5H, m), 6.34 (2H, t), 3.40 (2H, t), 2.82 (2H, t), 1.64−1.47 (2H, m). ^{13}C NMR (75 MHz, $CDCl_3$): δ (ppm) = 177.19, 137.93, 129.11, 128.05, 126.13, 47.31, 45.20, 43.22. FT-IR: 3064 (C═C−H str), 2946 (C−H asym str), 2877 (C−H sym str), 1770 (C═O), 1594 (C═C str), 1454 (C−H def), 1382 (═CH− def), 1329 (C−H def), 1289 (C−H def), 1188 (C−N str), 975 (C−C skel), 799 cm^{-1} (C═C−H def).

Metathesis Polymerizations of Monomers. Polymerizations were carried out in glass vials under a dry nitrogen atmosphere at 60 °C. Polymerizations were terminated by adding benzaldehyde under a nitrogen atmosphere. After cooling, the solutions were poured into an excess of methanol. The polymers were purified by solubilization in chloroform containing a few drops of 1 N HCl and precipitation into methanol, and they were further dried in a vacuum oven at 40 °C to constant weight.

Polymers Synthesis. *Poly(N-1-adamantyl-exo-norbornene-5,6-dicarboximide*) (*PAdNDI, M1).* 1 g (3.36 mmol) of **3a** and 0.033 g (0.33 mmol) of $(PPh_3)_2Cl_2Ru$═C═CH(*t*-Bu) were stirred in 3.4 mL of chlorobenzene at 60 °C for 8 h. The polymer obtained (Figure 4) was soluble in chloroform, toluene, and dichloromethane. ^{1}H NMR (300 MHz, $CDCl_3$): δ (ppm) = 5.67 (2H, s, trans), 2.76 (2H, s), 2.61 (2H, s), 2.35 (6H, s), 2.33 (3H, s), 1.68−1.64 (8H, d**)**. ^{13}C NMR (75 MHz, $CDCl_3$): δ (ppm) = 179.79, 133.90 (cis), 132.05 (trans), 60.63, 50.73, 46.33, 41.70, 39.25, 36.15, 29.71. FT-IR: 3038, 2924, 2855, 1768, 1700, 1665, 1455, 1372, 1340, 1304, 1194, 971, 762, 748 cm^{-1}.

Poly(N-cyclohexyl-exo-norbornene-5,6-dicarboximide)(*PChNDI, M2).* The polymerization procedure described above was used. ^{1}H NMR (300 MHz, $CDCl_3$) (Figure 5): δ (ppm) = 5.73 (2H, s**),** 3. 98 (1H, m), 2.92 (2H, d), 2.66 (2H, d), 2.14−2.11 (2H, d), 1.80−1.58 (6H, m), 1.27 (4H, m). ^{13}C NMR (75 MHz, $CDCl_3$): δ (ppm) = 178.49, 132.05 (trans), 51.29, 50.63, 46.10, 42.00, 28.73, 25.81, 25.07. FT-IR: 3036, 2934, 2893, 1768, 1700, 1665, 1452, 1370, 1346, 1304, 1297, 1186, 987, 762, 748 cm^{-1}.

Poly(N-phenyl-exo-norbornene-5,6-dicarboximide) (*PPhNDI, M3).* Poly(PhNDI) was prepared by a similar procedure as above for **3a**. ^{1}H NMR (300 MHz, $CDCl_3$): δ (ppm) = 7.44−7.25 (5H, m), 5.78 (2H, s), 3.13 (2H, s), 2.86 (2H, s), 2.20 (1H, s), 1.68 (1H, s). ^{13}C NMR (75 MHz, $CDCl_3$): δ (ppm) = 177.19, 132.33, 129.01, 128.22, 126.34, 50.31, 46.20, 42.22. FT-IR: 3034, 2930, 2877, 1775, 1594, 1459, 1385, 1329, 1290, 1165, 980, 790 cm^{-1}.

Copolymers Synthesis. The monomer **3a** was copolymerized with NB using $(PPh_3)_2Cl_2Ru$═C═CH(*t*-Bu), utilizing a similar procedure as above for **3a.** ^{1}H NMR (300 MHz, $CDCl_3$): δ (ppm) = 5.69 (2H, m, trans), 5.51 (2H, m, cis), 5.32 (2H, s, trans), 5.18 (2H, s, cis), 2.71−2.36 (12H, m), 2.07 (3H, s), 1.85−1.61 (10H, m), 1.33 (4H, m), 1.04 (4H, m). ^{13}C NMR (75 MHz, $CDCl_3$): δ (ppm) = 179.96, 133.90 (cis) 132.05 (trans)**,** 60.91, 50.98, 46.45, 43.11, 41.36, 39.27, 38.39, 36.18, 32.19, 29.74. FT-IR: 3027, 2934, 2860, 1766, 1665, 1452, 1370, 1346, 1187, 970, 786 cm^{-1}.

The glass transition temperatures of the M1, M2, M3, M4, M5, and M6 polymers measured with a DSC scanning calorimeter were respectively 271, 129, 233, 117, 202, and 80 °C.

Results

Some membranes exhibit a rather low permeability to certain gases that in some circumstances difficult to know whether steady-state conditions have been reached. To circumvent this problem, the equation

$$p(t) = 0.2786\frac{p_0 ALST}{V}\left(\frac{Dt}{L^2} - \frac{1}{6} - \frac{2}{\pi^2}\sum_{n=1}^{\infty}\frac{(-1)^n}{n^2} \times \exp\left(-\frac{Dn^2\pi^2 t}{L^2}\right)\right) \quad (1)$$

resulting from the integration of Fick's second law,[32] using appropriate boundary conditions, was fitted to the experimental results. In this equation $p(t)$ and p_0 which denote the pressures of gas in the downstream and upstream chambers, respectively, are given in cmHg, A and L which represent the area and thickness of the

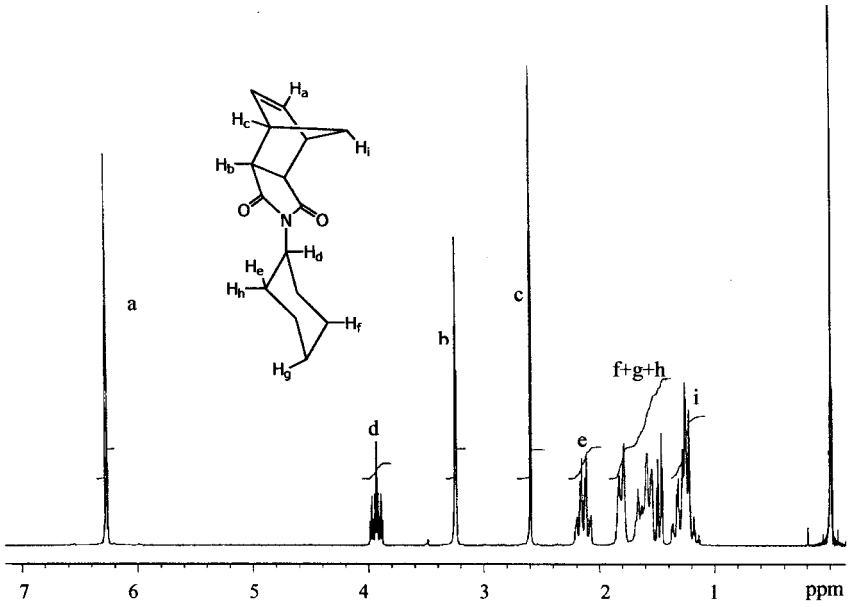

Figure 3. ^{1}H NMR spectrum of *N*-cyclohexyl-*exo*-norbornene-5,6-dicarboximide.

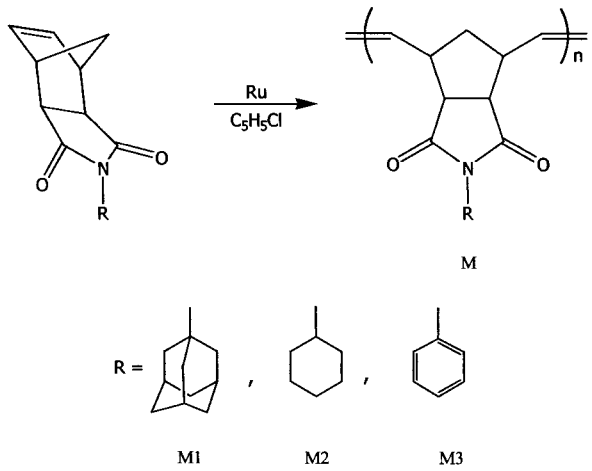

Figure 4. Synthesis of polymers via ROMP.

membrane in cm^2 and cm, respectively, the volume of the downstream chamber, V, in cm^3, the solubility coefficient of the gas, S, in cm^3 (STP)/(cm^3 cmHg), and D, the diffusion coefficient, in cm^2/s. Illustrative plots showing the fitting of eq 1 to the experimental values of the less permeable gas in the membrane M4, ethane, are represented in Figure 6.

All curves exhibit a transient zone followed by a region at long times where the pressure of the downstream chamber is a linear function of time. Once steady-state conditions are reached, eq 1 can be written as

$$p(t) = 0.2786\frac{p_0ALST}{V}\left(\frac{Dt}{L^2} - \frac{1}{6}\right) \qquad (2)$$

Plots of $p(t)$ against t in the steady state are straight lines intercepting the abscissa axis at $(D\theta/L^2) - {}^1/_6 = 0$, where θ is the time lag. Therefore, the diffusion coefficient can be obtained from the expression[33]

$$D = \frac{L^2}{6\theta} \qquad (3)$$

Errors Δ involved in the determination of D by the time lag method were obtained by means of the following expression

$$\Delta = \left(\frac{|L\epsilon(L)|}{3\theta} + \frac{|\epsilon(\theta)|L^2}{6\theta^2}\right)/D \qquad (4)$$

For most gases the error involved in the determination of the diffusion coefficient was less than 10%. However, for ethane and ethylene the error may be of the order of 25%.

By considering that the permeability coefficient, P, is the solubility coefficient times the diffusion coefficient ($P = DS$), its value can be obtained from eq 2 by means of the expression

$$P = 3.59\frac{VL}{p_0AT}\lim_{t\to\infty}\frac{\mathrm{d}p(t)}{\mathrm{d}t} \qquad (5)$$

Here P is given in barrers {1 barrer = [10^{-10} cm^3 (STP) cm/(cm^2 scmHg)]} provided that p_0 and $p(t)$ are given in cmHg and the rest of magnitudes in cgs units. The values of D obtained from eq 3 were compared with those determined by fitting eq 1 to the experimental results in order to know whether steady-state conditions were reached. As an example, the values obtained for the diffusion and permeability coefficients of ethane, directly calculated from the curve $p(t)$ vs t in the membrane M4, were 0.14 barrers and 4.7 $\times$ 10^{-9} cm^2/s, respectively. These values compare very favorably with those of 0.15 barrers and 4.0 $\times$ 10^{-9} cm^2/s obtained by fitting eq 1 to the experimental results. Even better agreement was found for the transport coefficients of the other gases in the different membranes.

Values of the permeability coefficient of the gases in the membranes are given in Table 1. An inspection of the table shows that all the membranes exhibit nearly the same behavior as far as the permeability of gases is concerned. Thus, hydrogen has the highest permeability coefficient followed by CO_2 and O_2, whereas the permeability coefficients of nitrogen, carbon monoxide, methane, and ethylene have nearly the same value.

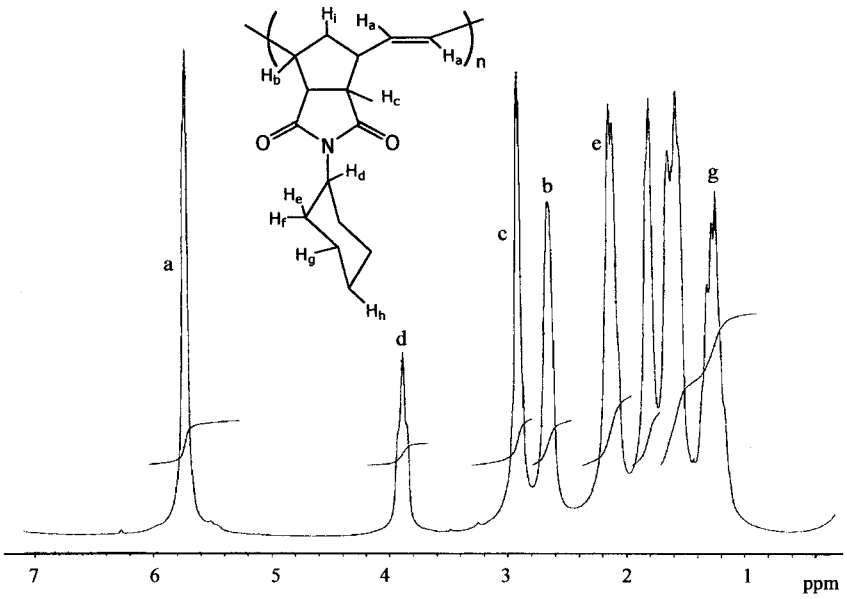

Figure 5. ^{1}H NMR spectrum of poly(*N*-cyclohexyl-*exo*-norbornene-5,6-dicarboximide).

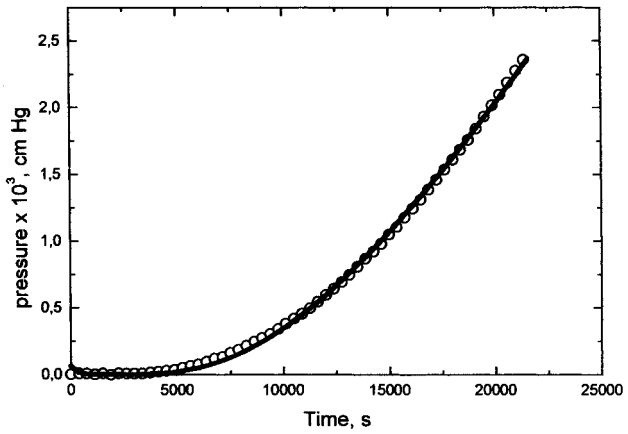

Figure 6. Experimental (circles) and calculated (continuous line) values of the pressure of ethane in the downstream chamber as a function of time.

Table 1. Permeability Coefficients in barrers of Different Gases in the Membranes Used in This Study

gas	M1	M2	M3	M4	M5	M6
H_2	12.8	16.1	11.0	10.7	18.2	12.2
O_2	1.59	2.13	1.44	1.21	1.92	1.40
N_2	0.50	0.61	0.31	0.22	0.60	0.43
CO	0.51	1.04	0.52	0.37	0.92	0.54
CO_2	8.39	18.11	11.44	5.11	8.13	
CH_4	0.58	1.12	0.54	0.42	0.96	0.60
C_2H_6	0.07	0.13	0.09	0.14	0.41	
C_2H_4	0.48	0.99	0.58	0.48	0.58	

Therefore, $P(H_2) \gg P(CO_2) > P(O_2) > P(N_2) \cong P(CO) \cong P(C_2H_4) \cong P(CH_4) > P(C_2H_6)$.

The values of the permeability coefficient show a significant dependence on the fine chemical structure of the membrane. The largest and lowest permeability coefficients of hydrogen occur in the M5 and M4 membranes, respectively. In general, the permeability of hydrogen in the membranes follows the trends $P(H_2, M5) > P(H_2, M2) > P(H_2,M1) \cong P(H_2, M6) > P(H_2, M3) \cong P(H_2,M4)$, where $P(H_2,Mi)$ represents the permeability coefficient of hydrogen in the membrane M*i*. The permeability coefficient of the other gases may not follow similar trends as hydrogen.

Table 2. Diffusion Coefficients, in 10^{-8} cm^2/s, of Different Gases in the Membranes Used in This Study

gas	M1	M2	M3	M4	M5	M6
H_2	160	212	132	244	323	2060
O_2	6.4	10.4	6.3	11.2	5.8	8.3
N_2	3.3	3.4	2.2	2.2	1.0	0.6
CO	2.0	2.8	1.4	3.2	1.3	1.4
CO_2	2.4	3.4	1.8	3.6	2.1	
CH_4	0.9	1.7	0.7	1.1	0.8	0.6
C_2H_6	0.7	1.7	0.4	0.5	0.7	
C_2H_4	0.8	0.8	0.3	0.5	0.3	

Values of the diffusion coefficient are presented in Table 2. It can be seen that hydrogen may exhibit diffusion coefficients 2 orders of magnitude or higher than those of the other gases. The high permeability of hydrogen in the membranes is mainly due to the high value of *D* that overcomes the rather low solubility of the gas in these materials. Independent of the type of membrane, the diffusion coefficient follows the trends $D(H_2) > D(O_2) > D(CO_2) \cong D(N_2) \cong D(CO) \cong D(CH_4) > D(C_2H_4) \cong D(C_2H_6)$. As for the effect of the structure of the membranes on the diffusion coefficient of hydrogen, the results indicate that $D(H_2,M6) > D(H_2,M5) > D(H_2,M4) > D(H_2,M2) > D(H_2,M1) > D(H_2,M3)$. This trend may not be hold for other gases.

The apparent solubility coefficient is given by

$$S = \frac{P}{D} \tag{6}$$

Carbon dioxide and ethylene are the gases with higher solubility, whereas hydrogen, which has the highest diffusion coefficient, turns out to have the lowest solubility coefficient. The value of *S* for hydrogen may be 2 orders of magnitude lower than the solubility coefficient of carbon dioxide. For example, the apparent solubility coefficients of H_2 and CO_2 in the membrane M1 are respectively 8.0×10^{-4} cm^3 (STP)/(cm^3 cmHg) and 3.5×10^{-2} in the same units. In general, $S(CO_2) > S(C_2H_4) > S(CH_4) > S(CO) > S(O_2) \cong S(N_2) > S(C_2H_6) > S(H_2)$. The relatively high value of the solubility coefficient of ethylene (6.0×10^{-3} cm^3 (STP)/(cm^3 cmHg)) in comparison with that of ethane (1.0×10^{-3} cm^3 (STP)/(cm^3 cmHg) is responsible for the relatively high perme-

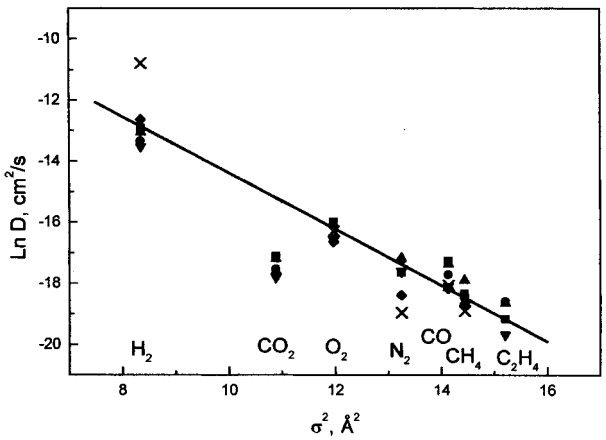

Figure 7. Natural logarithms of the diffusion coefficients of the gases as a function of the squares of their kinetic diameters for different membranes: (●) M1, (▲) M2, (▼) M3, (■) M4, (♦) M5, and (×) M6.

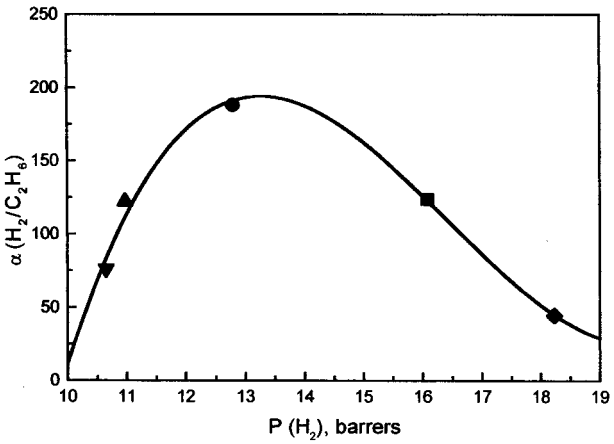

Figure 8. Experimental results of the permselectivity coefficient of hydrogen with respect to ethane represented as a function of the permeability of hydrogen in the membranes: (●) M1; (■) M2; (▲) M3; (▼) M4; (♦) M5.

ability coefficient of the unsaturated hydrocarbon in comparison with that of the saturated one.

Discussion

In the glassy state, molecules of diffusant spend a significant interval of time erratically moving in cavities where they are confined without contributing to the diffusive process. Although micro-Brownian motions are frozen in glassy molecular chains, fluctuations occur that may give rise to the formation of channels through which molecules slip to a neighboring cavity. Successful slippage requires not only an appropriate velocity of the molecules in the cavity next to the channel but also the radius of the channel to be larger than the radii of diffusant molecules. Therefore, it would be expected that, aside from polar interactions, diffusant molecules of larger radius should have lower diffusion coefficients. Values of the diffusion coefficient are plotted as a function of the radii of the diffusants in Figure 7. The plots show rather good concordance between the values of D and the kinetic diameter of the permeant molecules in the sense that D decreases as the radius increases. The values of the diffusion coefficient lie fairly well in a straight line except those corresponding to carbon dioxide that fall far below the regression line. The size of a gas diffusant molecule is estimated from the Lennard-Jones collision diameter (σ_c), determined on the basis of the molecular interactions of a gas, and the kinetic diameter (σ_k) which is close to the molecular sieving dimension of the molecule.[34,35] The former and latter parameters are widely accepted correlation parameters for diffusivities in the rubbery state and in the glassy state, respectively. The two diameters are nearly similar except for CO_2, for which the values of (σ_k) and (σ_c) are 3.30 and 4.00 Å, respectively. The correlation shown in Figure 7 is not much better if the diameter of carbon dioxide is taken to be as $(\sigma_k\sigma_c)^{1/2} =$ 3.63 Å. Therefore, repulsive interactions between the polar CO_2 and the polar matrices presumably delay the diffusion of the gas through the membranes.

Double bonds in the molecular chains confer rigidity to them alleviated by motions about two single bonds located in the structural unit. Conformational transitions on the cyclopentyl moieties that hinder chain packing cannot be ruled out. However, the polymers used in this study exhibit rather low permeability in comparison with other glassy polymers containing bulky substituted groups in their structure.[36] It is noteworthy that the M2 membrane is more permeable than the M1, although the adamantyl group should hinder chain packing more efficiently than the cyclohexyl group.

The permselectivity efficiency of a membrane to the transport of gas A with respect to gas B is defined as

$$\alpha(\mathrm{A/B}) = \frac{P(\mathrm{A})}{P(\mathrm{B})} = \frac{D(\mathrm{A})}{D(\mathrm{B})}\frac{S(\mathrm{A})}{S(\mathrm{B})} \qquad (7)$$

As was indicated in the Introduction, membranes are commonly used to separate hydrogen from both hydrocarbons and nitrogen in petrochemical processes. Let us discuss briefly the performance of these membranes regarding the permselectivity of hydrogen with respect to ethane, ethylene, methane, and carbon monoxide. A clear correlation between permselectivity and permeability is not clearly seen. Actually, the rule according to which the higher is the permeability the lower is the permselectivity does not seem to hold for $\alpha(H_2/C_2H_6)$. As shown in Figure 8, the permselectivity coefficient of hydrogen with respect to ethane increases as the permeability coefficient of hydrogen in the membranes increases, reaching a maximum for the membrane M1, and then decreases. As was indicated above, the diffusive process is responsible for the elevated permselectivity of the membranes toward hydrogen. Actually, the high diffusion coefficient of hydrogen overcomes the poor solubility of this gas in the membranes.

Values of $\alpha(H_2/N_2)$, $\alpha(H_2/CO)$, $\alpha(H_2/CH_4)$, $\alpha(H_2/C_2H_4)$, and $\alpha(H_2/O_2)$ are plotted as a function of the permeability coefficient of hydrogen in Figure 9. The values of $\alpha(H_2/C_2H_6)$, $\alpha(H_2/CH_4)$, and $\alpha(H_2/N_2)$ for the M1, M2, and M3 membranes are much higher than those reported for poly(vinyltrimethylsilane), poly(trimethylsilylnorbornene), and fluorine-containing ring-opened polynorbornenes.[22,23] It is worth noting that the membrane M4 is highly selective to hydrogen with respect to nitrogen. The values of $\alpha(H_2/CO)$, $\alpha(H_2/CH_4)$, and $\alpha(H_2/C_2H_4)$ are quite similar, and they do not show a clear dependence on the type of membrane.

The values of $\alpha(H_2/CO_2)$ lie in the interval 0.9−2.1 although the results obtained for $D(H_2)/D(CO_2)$ are 67, 62, 73, 68, and 154, respectively, in the membranes M1, M2, M3, M4, and M5. However, the solubility coefficient of CO_2 is significantly higher than that of H_2, the values of $S(CO_2)/S(H_2)$ being 44, 70, 76, 32, and 70, respectively,

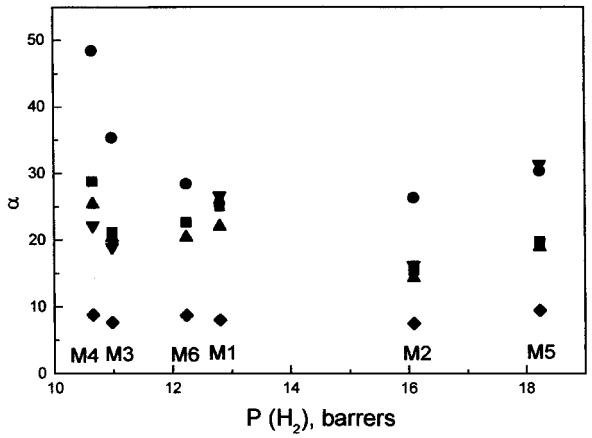

Figure 9. Variation of the (●) $\alpha(H_2/N_2)$, (■) $\alpha(H_2/CO)$, (▲) $\alpha(H_2/CH_4)$, (▼) $\alpha(H_2/C_2H_4)$, and (♦) $\alpha(H_2/O_2)$ with the permeability of hydrogen in different membranes.

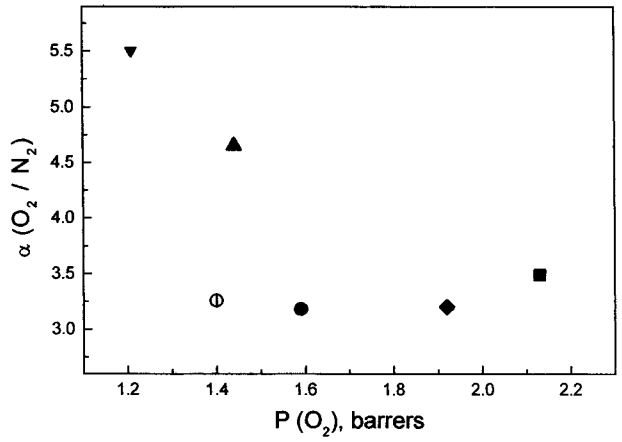

Figure 10. Permselectivity of oxygen with respect to nitrogen as a function of the permeability coefficient of oxygen in the membranes: (●) M1; (■) M2; (▲) M3; (▼) M4; (♦) M5; (Φ) M6.

in the membranes M1, M2, M3, M4, and M5. These facts explain the rather low permselectivity of hydrogen with respect to CO_2.

Values of the permselectivity of oxygen with respect to nitrogen are plotted as a function of the permeability coefficient of oxygen in Figure 10. The two membranes less permeable to both oxygen and nitrogen, M3 and M4, have the higher values of $\alpha(O_2/N_2)$, specifically 4.7 and 5.5, respectively. Since the apparent solubility coefficients of oxygen and nitrogen are similar in the M4 membrane, about 10^{-3} cm^3 (STP)/(cm^3 cmHg), the diffusive process is responsible for the high value of $\alpha(O_2/N_2)$ exhibited by this membrane. Actually, the ratio $D(O_2)/D(N_2)$ for the M4 membrane amounts to 5.1. In the case of the M3 membrane the values of $D(O_2)/D(N_2)$ and $S(O_2)/S(N_2)$ are 2.9 and 1.6, respectively. The values of the permselectivity of the other membranes are of the order of 3, less than the lower bound (4−5) admitted for commercial separation of oxygen from nitrogen.

Finally, it is important to know the permselectivity coefficients of CO_2 with respect to oxygen in films used in the package industry. The pertinent results show that the values of $\alpha(CO_2/O_2)$ are 8.5 and 7.9 for the membranes M2 and M3, respectively. The values of $\alpha(CO_2/O_2)$ for the M1, M4, and M-5 membranes are 5.3, 4.2, and 4.2, respectively.

Conclusions

Membranes prepared from poly(*N*-1-adamantyl-*exo*-norbornene-5,6-dicarboximide) (M1), poly(*N*-cyclohexyl-*exo*-norbornene-5,6-dicarboximide) (M2), poly(*N*-phenyl-*exo*-norbornene-5,6-dicarboximide) (M3), and *N*-(1-adamantyl)-*exo*-norbornene-5,6-dicarboximide/norbornene copolymers, with molar ratios 50/50 (M4), 70/30 (M5), and 30/70 (M6), exhibit permselectivity characteristics strongly dependent on the nature of the gases to be separated. The membranes M1, M2, and M3 display optimal characteristics for the separation of hydrogen from ethane. For the separation of hydrogen from methane all the membranes, except the M2, may be suitable. All the membranes exhibit rather high permselectivity for the separation of hydrogen from nitrogen, carbon monoxide, and ethylene. Only the membrane M3 and that prepared from M4 present values of $\alpha(O_2/N_2)$ that could make them suitable for the separation of oxygen from nitrogen. The other membranes show a rather bad performance for the separation of these gases. In general, the membranes exhibit permselectivity characteristics higher than those reported for other polynorbornenes. Although the results reported here are promising, more work is necessary to reach conclusions with respect to the capability of these materials to be used for separations in industrial processes. Attempts are being made to rationalize the solubility and diffusion coefficients reported in this work by simulation of these coefficients in terms of the chemical structure of the membranes.

Acknowledgment. We thank the CONACyT for generous support of this research with Contract NC-204. The authors thank Miguel Angel Canseco, Juan Manuel Garcia Leon, and Ruben Gavino for their assistance in thermal, GPC, and NMR analysis. Support of this work by the CAM (Spain) through Grant Bio-009-2000 is gratefully acknowledged.

References and Notes

(1) Flory, P. J. *Principles of Polymer Chemistry*; Cornell University Press: Ithaca, NY, 1953.
(2) Petropoulos, J. H. *Pure Appl. Chem.* **1993**, *65*, 219.
(3) Vieth, W. R.; Sladek, K. J. *J. Colloid Sci.* **1965**, *20*, 1014.
(4) Wen, W.-Y. *Chem. Soc. Rev.* **1993**, 117.
(5) Compañ, V.; Andrio, A.; López, M. L.; Alvarez, C.; Riande, E. *Macromolecules* **1997**, *30*, 3317.
(6) Compañ, V.; López-Lidón, M.; Andrio, A.; Riande, E. *Macromolecules* **1998**, *31*, 6984.
(7) Kesting, R. E.; Fritzsche, A. K. *Polymeric Gas Separation Membranes*; Wiley-Interscience: New York, 1993.
(8) Ohya, H.; Kudryavtsev, V. V.; Semenova, S. I. *Poliimide Membranes*; Gordon and Breach Publishers: Tokyo, 1996.
(9) Koros, W. J.; Fleming, G. K. *J. Membr. Sci.* **1993**, *83*, 1.
(10) Stern S. A. *J. Membr. Sci.* **1994**, *94*, 1.
(11) Al-Masri, M.; Kricheldorf, H. R.; Fritsch, D. *Macromolecules* **1999**, *32*, 7853.
(12) Gusev, A. A.; Müller-Plathe, F.; van Gunsteren, W. F.; Suter, U. V. *Adv. Polym. Sci.* **1994**, *116*, 207.
(13) Laguna, M.-F.; Saiz, E.; Guzmán, J.; Riande, E. *Macromolecules* **1998**, *31*, 7488.
(14) Laguna, M.-F.; Saiz, E.; Guzmán, J.; Riande, E. *J. Chem. Phys.* **1999**, *110*, 3200.
(15) López, M. M.; Saiz, E.; Guzmán, J.; Riande, E. *J. Chem. Phys.* **2001**, *115*, 6728.
(16) López, M. M.; Saiz, E.; Guzmán, J.; Riande, E. *Macromolecules* **2001**, *34*, 4999.
(17) Tlenkopatchev, M. A.; Miranda, E.; Canseco, M. A.; Gabiño, R.; Ogawa, T. *Polym. Bull.* **1995**, *34*, 385.
(18) Tlenkopatchev, M. A.; Fomine, S.; Fomina, L.; Gaviño, R.; Ogawa, T. *Polym. J.* **1997**, *29*, 622.
(19) Maya, V. G.; Contreras, A. P.; Canseco, M.-A.; Tlenkopatchev, M. A. *React. Funct. Polym.* **2001**, *49*, 145.

(20) Ivin, K. J.; Mol, J. C. In *Olefin Metathesis and Metathesis Polymerization*; Academic Press: San Diego, CA, 1997; Chapter 13.
(21) Paul, D. R.; Yampolskii, Yu. P. *Polymeric Gas Separation Membranes*; CRC Press: Boca Raton, FL, 1994.
(22) Bondar, V. I.; Kukharskii, Yu. M.; Yampolskii, Yu. P.; Finkelshtein, E. Sh.; Makovetskii, K. L. *J. Polym. Sci., Part B: Polym. Phys.* **1993**, *31*, 1273.
(23) Yampolskii, Yu. P.; Bespalova, N. B.; Finkelshtein, E. Sh.; Bondar, V. I.; Popov, A. V. *Macromolecules* **1994**, *27*, 2872.
(24) Yampolskii, Yu. P.; Finkelshtein, E. Sh.; Makovetskii, K. L.; Bondar, V. I.; Shantarovich, V. P. *J. Appl. Polym. Sci.* **1996**, *62*, 349.
(25) Dorkenoo, K. D.; Pfromm, P. H.; Rezac, M. E. *J. Polym. Sci., Part B: Polym. Phys.* **1998**, *36*, 797.
(26) Zhao, Ch-T.; Do Rosario Ribeiro, M.; de Pinho, M. N.; Subrahmanyan, V. S.; Gil, C. L.; de Lima, A. P. *Polymer* **2001**, *42*, 2455.
(27) Contreras, A. P.; Tlenkopatchev, M. A.; Ogawa, T.; Nakagawa, T. *Polym. J.* **2002**, *34*, 49.
(28) Kastner, K. F.; Calderon, N. J. *J. Mol. Catal.* **1982**, *15*, 47.
(29) Smith, T. A.; Aplin, R. P.; Maitlis, P. M. *J. Organomet. Chem.* **1985**, *291*, C13.
(30) Wakatsuki, Y.; Yamazaki, H.; Kumegawa, N.; Satoh, T.; Satoh, J. Y. *J. Am. Chem. Soc.* **1991**, *113*, 9604.
(31) Asrar, J. *Macromolecules* **1992**, *25*, 5150.
(32) Crank, J. *The Mathematics of Diffusion*; Oxford University Press: New York, 1975.
(33) Barrer, R. M. *Trans. Faraday Soc.* **1939**, *35*, 628.
(34) Breck, D. W. *Zeolite Molecular Sieves*; Wiley: New York, 1974; p 636.
(35) Costello, L. M.; Koros, W. J. *J. Polym. Sci., Part B: Polym. Phys.* **1994**, *32*, 701.
(36) Park, J. Y.; Paul, D. R. *J. Membr. Sci.* **1997**, *125*, 23.

MA011959P